Charge-State Conditional Operation of a Spin Qubit

I. van Weperen,[1,2] B. D. Armstrong,[1] E. A. Laird,[1,*] J. Medford,[1] C. M. Marcus,[1] M. P. Hanson,[3] and A. C. Gossard[3]

[1]*Department of Physics, Harvard University, Cambridge, Massachusetts 02138, USA*
[2]*Kavli Institute of Nanoscience, Delft University of Technology, 2600 GA Delft, The Netherlands*
[3]*Materials Department, University of California, Santa Barbara, California 93106, USA*

(Received 9 February 2011; published 15 July 2011)

We report coherent operation of a singlet-triplet qubit controlled by the spatial arrangement of two confined electrons in an adjacent double quantum dot that is electrostatically coupled to the qubit. This four-dot system is the specific device geometry needed for two-qubit operations of a two-electron spin qubit. We extract the strength of the capacitive coupling between qubit and adjacent double quantum dot and show that the present geometry allows fast conditional gate operation, opening pathways toward implementation of a universal set of gates for singlet-triplet spin qubits.

DOI: 10.1103/PhysRevLett.107.030506 PACS numbers: 03.67.Lx, 73.21.La

Advances in control of single electrons in quantum dots [1] have led to the prospect of using electron spin as a quantum bit (qubit) in quantum computation [2]. One formulation of the qubit uses singlet $|S\rangle = \frac{1}{\sqrt{2}}(|\uparrow\downarrow\rangle - |\uparrow\downarrow\rangle)$ and triplet $|T_0\rangle = \frac{1}{\sqrt{2}}(|\uparrow\downarrow\rangle + |\uparrow\downarrow\rangle)$ states [3] of two electrons in a double quantum dot (DQD) [Fig. 1(a)]. Most requirements for quantum computing [4] with this qubit have been met [5–8], including all electrical full single-qubit control [9]. Rotation about the z axis of the Bloch sphere [Fig. 1(a)] is governed by the exchange interaction between two spins, which can be controlled electrostatically near degeneracies of the charge arrangement of the two electrons. Rotation about the x axis is mediated by gradients of the Zeeman field, produced either by nuclear gradients [9] or by permanent magnets [10].

The electrostatic interaction between DQDs was identified theoretically to lead to a two-qubit interaction sufficient for universal quantum computation [11]. In this scheme, the control (C) DQD is configured to allow its spin configuration (S or T_0) to determine its charge state via Pauli blockade [12] of the charge transition from the singly occupied $(1, 1)$ to the doubly occupied $(0, 2)$ [or $(2, 0)$] configuration, where (N_L, N_R) are the absolute electron occupancies of the left and right QD. That is, rapid relaxation into the symmetric orbital ground state of $(0, 2)$ occurs only for the spin-antisymmetric singlet (S) state, while the spin-symmetric triplet (T_0) remains trapped in the $(1, 1)$ charge configuration. The resulting charge state of the control DQD in turn influences the rate of coherent state evolution in the target (T) DQD through the dependence of the exchange interaction on electrostatic tuning. The two-qubit operation is thus mediated by the charge configuration of the control DQD [Fig. 1(b)].

While electrostatically coupled proximal electron pairs constitute the main candidate for two-qubit operations for the singlet-triplet qubits, this system has not been realized or assessed experimentally to date. The present study realizes the relevant four-dot system and provides key parameters of the capacitive interaction. We further demonstrate controlled coherent operation of one DQD, operating as a singlet-triplet qubit, using the two-electron charge configuration of the other DQD. We find that the repositioning of a single electron in the fixed two-electron system is sufficient to control the evolution of a phase gate. We stress, however, that the performance of this two-qubit logic gate remains a future challenge.

A pair of DQDs were defined with Ti/Au depletion gates on a $GaAs/Al_{0.3}Ga_{0.7}As$ heterostructure with two-dimensional electron gas (2DEG) 110 nm below the surface [Fig. 2(a)]. 2DEG mobility was 2×10^5 cm^2 V^{-1} s^{-1} with electron density 2×10^{15} m^{-2}. Electron temperature was $\sim$150 mK. The $S = 1$ triplet states were separated using an external magnetic field $B_{\text{ext}} = 0.1$ T applied in the plane of the 2DEG.

Electron configurations in both DQDs were controlled by tuning the voltages applied to the plunger depletion gates $V^L_{C(T)}$ and $V^R_{C(T)}$, and were measured with proximal quantum point contact (QPC) sensors [13,14]. The control [target] DQD was tuned to the $(1, 1)_C$-$(0, 2)_C$ $[(1, 1)_T$-$(2, 0)_T]$ charge transition [Figs. 2(b) and 2(c)] where Pauli blockade was observed for both DQDs in both transport and charge sensing [15,16]. Voltage detuning

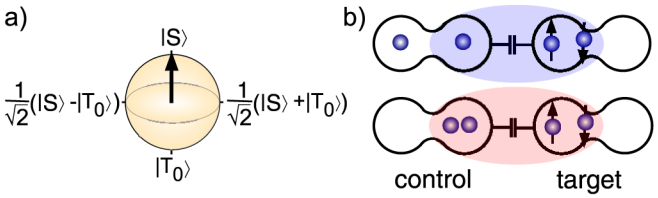

FIG. 1 (color online). (a) Bloch sphere representation of the singlet-triplet qubit, which is formed by the singlet S and $m_s = 0$ triplet T_0 electron spin states of two singly occupied quantum dots. (b) Electrostatic interaction between proximal double quantum dots (DQDs) alters the rate of coherent evolution in one DQD depending on the charge configuration of the other DQD.

axes ϵ_C and ϵ_T were defined along the $(1,1)_C$-$(0,2)_C$ and $(1,1)_T$-$(2,0)_T$ charge transitions of the control and target DQDs, as shown in Figs. 2(b) and 2(c) [17].

The strength of the capacitive interaction between DQDs defines a coupling strength, $E^0_{\rm cpl}$, given by the differential cross capacitance energy $E[(0,2)_C(2,0)_T] - E[(0,2)_C(1,1)_T] - \{E[(1,1)_C(2,0)_T] - E[(1,1)_C(1,1)_T]\}$, with $E[(N_L,N_R)_C,(N_L,N_R)_T]$ the energy of the system with charge configuration $(N_L,N_R)_C$ in the control DQD and $(N_L,N_R)_T$ in the target DQD. When the control DQD was tuned to the $(0,2)_C$ charge state, the $(1,1)_T$-$(2,0)_T$ charge transition of the target DQD shifted to a more positive detuning by an amount $\epsilon_{\rm cpl}$ [Fig. 2(d)]. This shift in detuning reflects an increased energy of the $(0,2)_C(2,0)_T$ state resulting from capacitive coupling between DQDs. The detuning voltage shift of 0.63 mV, when converted to energy based on finite-bias transport measurements, gives $E^0_{\rm cpl} = 23 \pm 3\ \mu$eV.

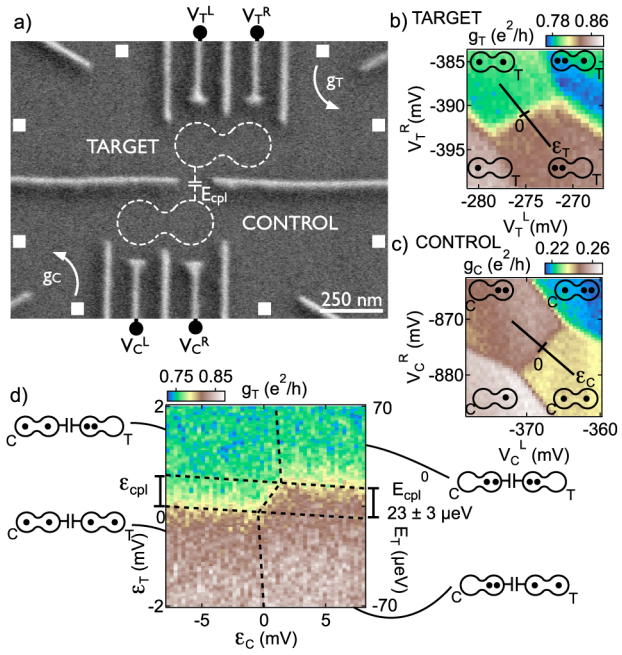

FIG. 2 (color online). (a) Micrograph of a device similar to the one measured. Gate voltages V_T^L and V_T^R (V_C^L and V_C^R) control the charge state of the target (control) DQD. Quantum point contacts (QPCs) with conductances g_T and g_C sense charge states of target and control DQDs. The DQDs are capacitively coupled by an electrostatic interaction $E_{\rm cpl}$. (b) [(c)] QPC conductance measured as a function of gate voltages V_T^L and V_T^R [V_C^L and V_C^R] dot shows distinct conductance levels g_T [g_C] for each electron configuration $(N_L,N_R)_T$ [$(N_L,N_R)_C$]. Detuning axes ϵ_T and ϵ_C for target and control DQD are indicated. (d) Voltage detuning ϵ_T of the target DQD as a function of the voltage detuning ϵ_C of the control DQD. The shift of the target detuning axis $\epsilon_{\rm cpl}$ that occurs when the occupancy of the control DQD changes is indicated on the left axis. The right axis shows the corresponding energy shift $E^0_{\rm cpl}$. The difference in conductance of the $(1,1)_T$ and $(2,0)_T$ occupancy between (b) and (d) is due to a difference in operating point of the QPC.

Coherent manipulation of the target qubit makes use of the dependence of the exchange energy J, the difference in energy between the singlet and triplet level, on detuning ϵ_T along the $(1,1)_T$-$(2,0)_T$ axis. When the charge state of the control DQD changes from $(1,1)_C$ to $(0,2)_C$, the detuning axis of the target qubit shifts from ϵ_T, with exchange energy $J(\epsilon_T)$, to $\epsilon_T - \epsilon_{\rm cpl}$, with reduced exchange energy $J(\epsilon_T - \epsilon_{\rm cpl})$, as shown in Fig. 3(a). The difference in exchange energy $J(\epsilon_T) - J(\epsilon_T\text{-}\epsilon_{\rm cpl})$ defines the detuning-dependent coupling strength $E_{\rm cpl}(\epsilon_T)$ [Fig. 3(b)], which we describe, following Taylor *et al.* [11,18] with the hybrid state $|\tilde{S}\rangle = \cos\theta|S\rangle + \sin\theta|S(2,0)\rangle$ on the lower branch of the anticrossing, where $\theta = \arctan[2\kappa(\epsilon - \sqrt{4\kappa^2+\epsilon^2})^{-1}]$ is the angle parametrizing the admixture, with interdot tunnel coupling $\kappa \sim 6\ \mu$eV (discussed below). With the control in $(0,2)_C$ and the target at θ_T, the detuning-dependent coupling strength is given by $E^0_{\rm cpl}\sin^2\theta_T$ [11]. When the target DQD is fully within $(2,0)_T$ (i.e., large positive ϵ_T), the shift by $\epsilon_{\rm cpl}$ results in an increase in the energy of the target state by the maximal coupling energy, $E^0_{\rm cpl}$.

To demonstrate charge-state conditional evolution, the target qubit must be manipulated before and after its interaction with the control qubit using a series of voltage pulses [Fig. 4(a)] applied to the plunger gates [5]. A Textronix AWG 520 was used for fast gate control, allowing ~1 ns pulse rise times. A singlet $S(2,0)$ was prepared in the $(2,0)_T$ charge state, after which it was adiabatically loaded into the superposition $\frac{1}{\sqrt{2}}(|S\rangle + |T_0\rangle)$ in $(1,1)_T$ [Fig. 4(b)]. Detuning was pulsed to a negative value ϵ_T^I

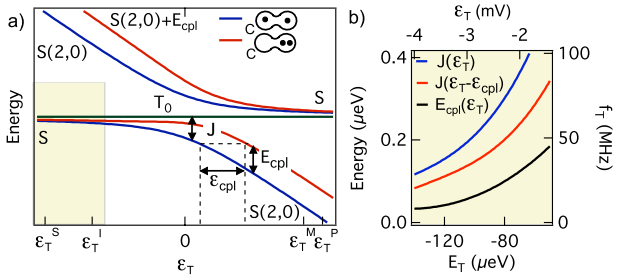

FIG. 3 (color online). (a) Energy diagram near the $(1,1)_T$-$(2,0)_T$ transition of the target DQD. Energy levels of the hybrid singlet state as a function of target detuning ϵ_T for $(1,1)_C$ [dark gray (blue) curve] and $(0,2)_C$ [light gray (red) curve] occupation of the control DQD. Detuning of the target qubit at which separation of the electrons in separate quantum dots ϵ_T^S, interaction of the two DQDs ϵ_T^I, measurement ϵ_T^M, and singlet preparation ϵ_T^P take place during coherent manipulation are indicated. The yellow area indicates detuning range considered in (b). (b) Singlet-triplet energy splittings and corresponding target qubit precession frequency f_T for control DQD occupation $(1,1)_C$ [dark gray (blue) curve] and $(0,2)_C$ [light gray (red) curve]. Difference in exchange energies, $E_{\rm cpl}(\epsilon_T)$ (black curve) determine the duration for conditional operation. Exchange energies obtained from fits to the data of Fig. 5, coupling energy from the model in Ref. [11].

where the singlet and T_0 triplet level were separated by an energy $J(\epsilon_T^I)$. Precession with frequency $h^{-1}J(\epsilon_T^I)$ occurred for an interaction time τ_I. Following adiabatic unloading, spin-dependent tunneling into $(2,0)_T$ was used to determine the singlet component of the qubit P_T^S from an average measurement of QPC conductance over many repeated cycles. With the control DQD in $(0,2)_C$ the precession frequency was reduced to $h^{-1}J(\epsilon_T^I - \epsilon_{\rm cpl})$, while no such reduction was observed when the control was in $(1,1)_C$.

The oscillation of singlet probability with interaction time τ_I in Fig. 4(c) demonstrates coherent precession of the target qubit. The target precessed more slowly when the occupancy of the control DQD was $(0,2)_C$ (detuning $\epsilon_C = 2.5$ mV) than with control DQD occupancy $(1,1)_C$ ($\epsilon_C = -2.5$ mV) [Fig. 4(e)]. Precession frequency f_T as a function of ϵ_C [Figs. 4(c) and 4(d)] shows that the decrease occurs near $\epsilon_C = 0$ mV, where the charge state of the control DQD changed from $(1,1)_C$ ($\epsilon_C < 0$) to $(0,2)_C$ ($\epsilon_C > 0$). Away from $\epsilon_C = 0$ mV no noticeable change in frequency was observed, ruling out direct effects of the gate voltages V_C^L and V_C^R on the precession rate, which would presumably instead appear as a continuous change in precession frequency along ϵ_C. The coupling precession, the difference in precession rate $h^{-1}E_{\rm cpl}(\epsilon_T^I)$ between both control DQD configurations, constitutes a qubit operation conditional on the charge configuration of the two electrons in the control DQD. Target coherence times were longer for control in $(0,2)_C$ compared to $(1,1)_C$, consistent with gate-noise-induced dephasing with roughly constant quality factor [5]. No significant increase in decoherence at the control charge transition between $(0,2)_C$ and $(1,1)_C$ is observed.

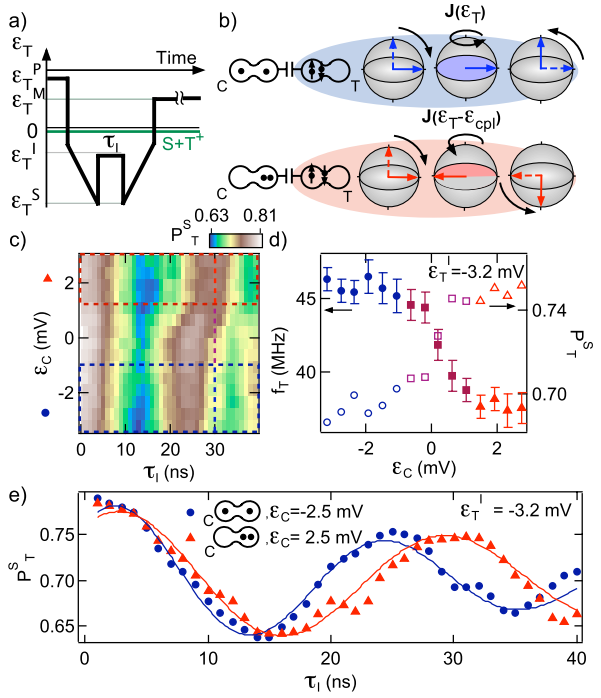

FIG. 4 (color online). (a) Pulse sequence used in coherent manipulation of the target qubit. Target detuning ϵ_T^P for singlet preparation, ϵ_T^S for adiabatic loading of the singlet-triplet superposition state, ϵ_T^I for exchange and coupling interaction, and ϵ_T^M for measurement are indicated. (b) Target qubit evolution in Bloch sphere representation during adiabatic loading, coherent exchange precession, and adiabatic unloading. Moving an electron in the control DQD towards the target qubit shifts the target qubit detuning from ϵ_T to $\epsilon_T - \epsilon_{\rm cpl}$, causing slower precession. (c) Singlet probability of the target qubit P_T^S as a function of interaction time τ_I and control DQD detuning ϵ_C, with $\epsilon_T^I = -3.2$ mV. A shift in period occurs around $\epsilon_C = 0$ mV, where control DQD occupancy changes. Dashed rectangles indicate the detuning ranges used in (e). Cut at $\tau_I = 30$ ns is shown in (d) (right axis). (d) Left axis: Precession frequency of the target qubit f_T as function of detuning, from (c). Right axis: Singlet probability for interaction time $\tau_I = 30$ ns, vertical cut from (c). (e) Precession of the target qubit as a function of interaction time τ_I at control DQD detuning $\epsilon_C = -2.5$ mV [blue dots, control DQD in $(1,1)_C$] and $\epsilon_C = 2.2$ mV [red triangles, control DQD in $(0,2)_C$]. Nonzero phase of the damped cosine fits at $\tau_I =$ is due to the rise time of the coupling voltage pulse.

Figure 5(a) demonstrates a conditional phase flip in ~30 ns. After that time, the initial target state $\frac{1}{\sqrt{2}}(|S\rangle + |T_0\rangle)$ has evolved through 3π to $\frac{1}{\sqrt{2}}(|S\rangle - |T_0\rangle)$

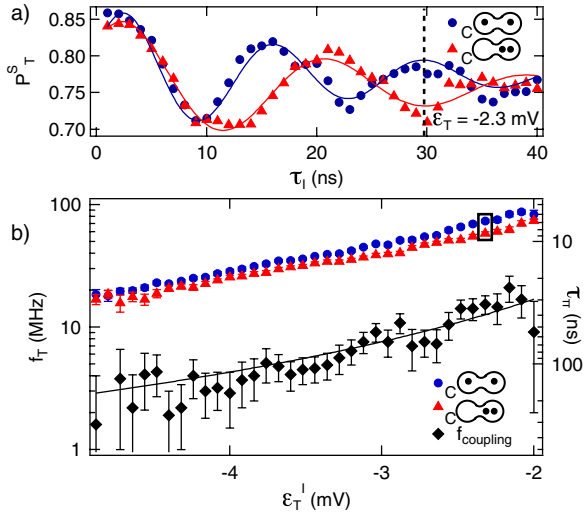

FIG. 5 (color online). (a) Singlet probability of the target qubit P_T^S as a function of interaction time τ_I. After 30 ns (indicated with the dashed line) a 4π rotation of the target qubit has been performed when the control DQD is in the $(1,1)_C$ charge state (blue dots and fit to the data), while a 3π rotation is performed when the control DQD is in the $(0,2)_C$ charge state (red triangles and fit to the data). This corresponds to a phase flip of the target qubit conditional on the occupancy of the control DQD. (b) Precession frequency f_T as a function of target qubit detuning ϵ_T with the control DQD in the $(1,1)_C$ (blue circles, detuning $\epsilon_C = -8.1$ mV) and $(0,2)_C$ (red triangles, detuning $\epsilon_C = 5.4$ mV) charge state. Coupling frequency is the difference frequency between both data sets. Black curve is a fit to the coupling frequency data with the tunnel coupling as only free parameter. The two data points in the box correspond to the oscillations in (a). The right axis shows the interaction time required for a phase flip.

with control in $(0, 2)_C$. With the control in $(1, 1)_C$, the target evolved through 4π to its initial state. Figure 5(b) shows the precession frequency f_T increasing with increasing target detuning, reflecting an increase of $S(2, 0)$ component in the hybrid singlet state with detuning. A fit to the measured $E_{\mathrm{cpl}}(\epsilon_T^I)$ with the theoretical $\sin^2\theta_T$ relation of coupling frequency to detuning was made. The coupling strength, E_{cpl}^0, used in this fit was found from the shift in detuning voltage needed to match the precession frequency of the target when the control DQD was in $(0, 2)_C$ to the precession frequency with the control in $(1, 1)_C$. A detuning shift of -0.32 mV corresponds to a coupling energy E_{cpl}^0 of 11 μeV [19]. Excellent agreement between the data and model for the detuning-dependent precession frequency is found, using a value of tunnel coupling $\kappa = 5.6 \pm 0.3$ μeV in the target DQD as a single fit parameter.

The fastest measured time scale for conditional precession, $\tau_\pi^{\mathrm{cond}} \sim \pi\hbar[E_{\mathrm{cpl}}(\epsilon_T)]^{-1}$, defined as the time for a phase lag of π to accumulate during the coherent evolution of the target qubit with control DQD charge configuration $(0, 2)$ compared to the evolution with $(1, 1)_C$ control DQD occupancy, is 20–30 ns [Fig. 5(b), right axis), corresponding to $E_{\mathrm{cpl}}(\epsilon_T) \sim 0.01 E_{\mathrm{cpl}}^0$. This value can be used to infer the speed of a two-qubit singlet-triplet gate, where the spin state of the control qubit with θ_C influences the spin evolution of the target qubit. In this situation the coupling strength is given by $E_{\mathrm{cpl}}^0 \sin^2\theta_T \sin^2\theta_C$, giving a time scale for the controlled phase two-qubit gate of $\tau_\pi^{\mathrm{contr}} \sim \pi\hbar[E_{\mathrm{cpl}}(\epsilon_T, \epsilon_C)]^{-1}$. If both control and target qubits were operated in the range of detunings used here, this characteristic time would be $\sim$100 times longer than the conditional precession time we measure, giving ~ 3 μs. On the other hand, operating the target and control near zero detuning, with $E_{\mathrm{cpl}}^0 \sim 20$ μeV (for the present device geometry), yields a more favorable value, $\tau_\pi^{\mathrm{contr}} \sim 0.4$ ns. Comparison with multiecho coherence times of order 100 μs [7,8] for individual singlet-triplet qubits suggests that the coupling strength obtained with the current device geometry, operated at small detunings, should be adequate for two-qubit gate operations. A larger coupling strength is, however, preferable to achieve high fidelity two-qubit operations, as working at small singlet components (i.e., at more negative detuning) is expected to yield smaller dephasing errors [11]. Device geometries that further enhance capacitive coupling are under development currently.

We thank T. Christian for valuable discussion and carrying out preliminary studies. This work was supported by the Intelligence Advance Research Projects Agency (IARPA) Multi-Qubit Coherent Operations (MQCO) Program, the Defence Advance Research Projects Agency (DARPA) Quantum Entanglement Science and Engineering Technologies (QuEST) Program, and the National Science Foundation (NSF) through the Materials World Network (MWN) and the Harvard Nanoscale Science and Engineering (NSEC). Devices were fabricated at Harvard University at the Center for Nanoscale Systems (CNS), part of the NSF National Nanofabrication Infrastructure Network (NNIN).

*Present address: Kavli Institute of Nanoscience, Delft University of Technology, 2600 GA Delft, The Netherlands.

[1] R. Hanson *et al.*, Rev. Mod. Phys. **79**, 1217 (2007).
[2] D. Loss and D. P. DiVincenzo, Phys. Rev. A **57**, 120 (1998).
[3] J. Levy, Phys. Rev. Lett. **89**, 147902 (2002).
[4] D. P. DiVincenzo, Fortschr. Phys. **48**, 771 (2000).
[5] J. R. Petta *et al.*, Science **309**, 2180 (2005).
[6] C. Barthel *et al.*, Phys. Rev. Lett. **103**, 160503 (2009).
[7] H. Bluhm *et al.*, Nature Phys. **7**, 109 (2010).
[8] C. Barthel *et al.*, Phys. Rev. Lett. **105**, 266808 (2010).
[9] S. Foletti *et al.*, Nature Phys. **5**, 903 (2009).
[10] M. Pioro-Ladrière *et al.*, Nature Phys. **4**, 776 (2008).
[11] J. M. Taylor *et al.*, Nature Phys. **1**, 177 (2005).
[12] K. Ono *et al.*, Science **297**, 1313 (2002).
[13] M. Field *et al.*, Phys. Rev. Lett. **70**, 1311 (1993).
[14] J. M. Elzerman *et al.*, Phys. Rev. B **67**, 161308(R) (2003).
[15] A. C. Johnson *et al.*, Phys. Rev. B **72**, 165308 (2005).
[16] See Supplemental Material at http://link.aps.org/supplemental/10.1103/PhysRevLett.107.030506 for a description of the few electron regime of the control DQD and transport measurements of Pauli blockade in both DQDs.
[17] Conversion of voltage detuning ϵ to energy detuning E is performed by multiplication of ϵ with electron charge e and a lever arm. This lever arm is obtained in finite-bias transport measurements from the size of bias triangles in plunger gate voltage space. This procedure is described in the supplemental material [16].
[18] J. M. Taylor *et al.*, Phys. Rev. B **76**, 035315 (2007).
[19] The change of coupling strength between the measurement of Fig. 2(d) and that of Fig. 5 is likely due to a slow drift in the quantum dot system, resulting in a change in position of the quantum dots and in their mutual coupling.